Development 129, 2867-2878 (2002)
Printed in Great Britain © The Company of Biologists Limited 2002
DEV9829

Tiling of the *Drosophila* epidermis by multidendritic sensory neurons

Wesley B. Grueber, Lily Y. Jan and Yuh Nung Jan*

Howard Hughes Medical Institute, Departments of Physiology and Biochemistry, 533 Parnassus Avenue, Room U226, Box 0725, University of California, San Francisco, San Francisco, CA 94143-0725, USA
*Author for correspondence (e-mail: ynjan@itsa.ucsf.edu)

Accepted 2 April 2002

SUMMARY

Insect dendritic arborization (da) neurons provide an opportunity to examine how diverse dendrite morphologies and dendritic territories are established during development. We have examined the morphologies of *Drosophila* da neurons by using the MARCM (mosaic analysis with a repressible cell marker) system. We show that each of the 15 neurons per abdominal hemisegment spread dendrites to characteristic regions of the epidermis. We place these neurons into four distinct morphological classes distinguished primarily by their dendrite branching complexities. Some class assignments correlate with known proneural gene requirements as well as with central axonal projections. Our data indicate that cells within two morphological classes partition the body wall into distinct, non-overlapping territorial domains and thus are organized as separate tiled sensory systems. The dendritic domains of cells in different classes, by contrast, can overlap extensively. We have examined the cell-autonomous roles of *starry night* (*stan*) (also known as *flamingo* (*fmi*)) and *sequoia (seq)* in tiling. Neurons with these genes mutated generally terminate their dendritic fields at normal locations at the lateral margin and segment border, where they meet or approach the like dendrites of adjacent neurons. However, *stan* mutant neurons occasionally send sparsely branched processes beyond these territories that could potentially mix with adjacent like dendrites. Together, our data suggest that widespread tiling of the larval body wall involves interactions between growing dendritic processes and as yet unidentified signals that allow avoidance by like dendrites.

Key words: Dendrite development, Peripheral nervous system, Tiling, Dendritic arborization neurons, *Drosophila*

INTRODUCTION

Mature nervous systems contain enormous numbers of neurons, each one with its own unique dendritic field. A fundamental problem of neuronal development and morphogenesis is how, amidst such complexity of form, function and organization, do dendritic arbors acquire their proper morphologies and territories. Put another way, how are dendrites instructed when to grow and branch and when to stop.

Interactions with nearby neurons can provide cues to stop dendritic growth or to change the trajectory of growth (Perry and Linden, 1982; Scott and Luo, 2001; Jan and Jan, 2001). The phenomenon of 'tiling' appears to offer a particularly dramatic example of such interactions. Tiling, which has been studied most extensively in alpha ganglion cells of the mammalian retina (Wässle et al., 1981), refers to the complete but non-redundant innervation of a receptive area by dendrites of functionally uniform groups of neurons. Studies of the alpha ganglion cells identified two functionally distinct subpopulations, ON-center and OFF-center, with cell bodies arranged in independent mosaics across the retina (reviewed in Wässle and Boycott, 1991). Dendrites from each subpopulation fill in the space between the cell bodies completely but in doing so overlap minimally with other like dendrites. Consequently, each physiological type of cell covers every region of visual space with high economy (Wässle et al., 1981). With additional techniques for labeling different subsets of ganglion cells, it has become apparent that several other types [there are up to 15 (Masland, 2001)] are also organized as tiled systems (Wässle and Boycott, 1991). Thus, in the mammalian retina, tiling is a dominant theme in the organization of complex dendritic fields within 2D planes. Such an arrangement ensures complete and yet non-redundant representation of the sensory or presynaptic input for each physiological function being processed.

The rules of tiling suggest that subtype-specific cues can direct like dendrites to avoid each other and thereby establish non-overlapping territories. Consistent with this notion, depletion of a patch of retinal ganglion cells causes surrounding neurons to grow dendrites preferentially toward the voided area (Perry and Linden, 1982; Hitchcock, 1989). Lesion experiments have also demonstrated that growth occurs in a cell-class-specific manner (Weber et al., 1998), suggesting that a like-repels-like mechanism normally operates between dendrites. Such a scenario is further supported by the occurrence of cell-type-specific dendritic contacts between alpha cells, which could provide an opportunity for signaling via cell surface molecules or gap junctions (Lohmann and Wong, 2001). Despite strong experimental evidence for selective dendritic recognition and exclusion in the retina, the molecular mechanisms controlling territory avoidance by like dendrites are not known.

The peripheral nervous system (PNS) of insects is well

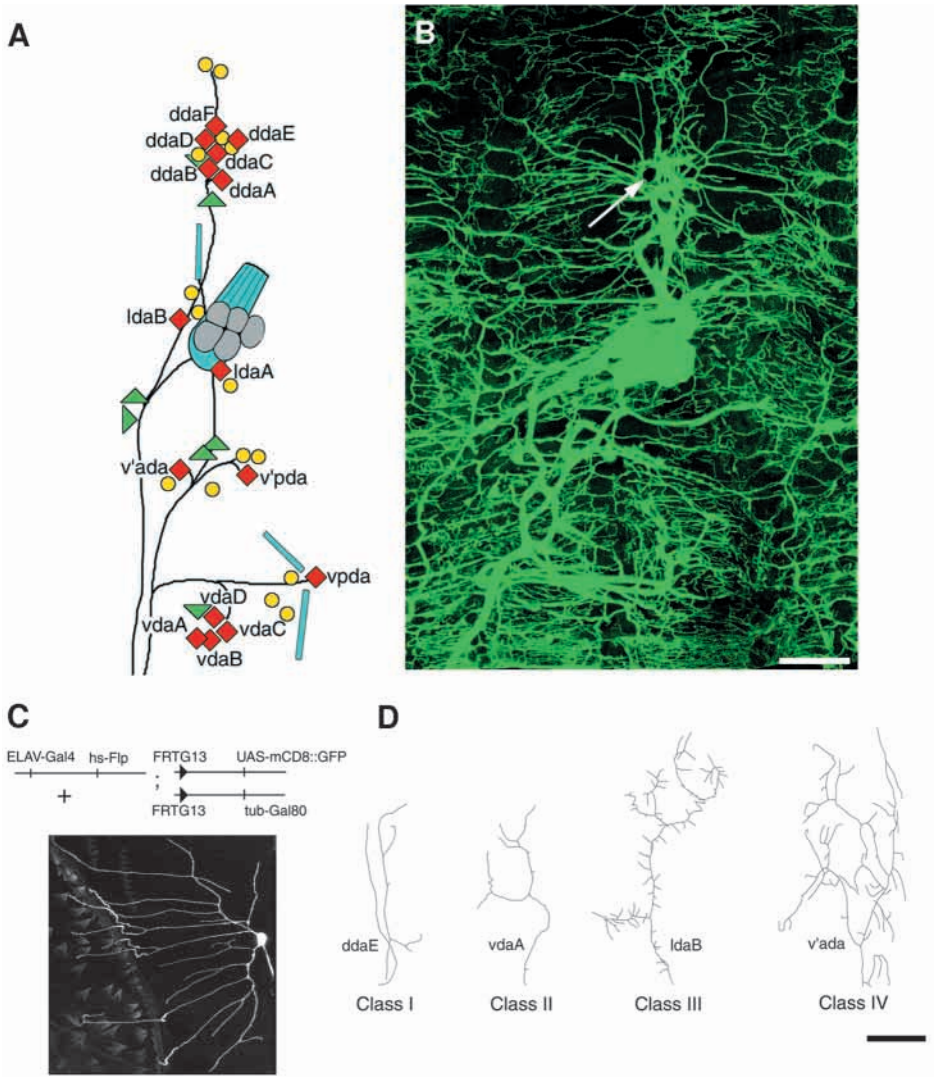

Fig. 1. Identification of peripheral dendritic arborization (da) neurons using the MARCM system.
(A) A diagram of the *Drosophila* abdominal peripheral nervous system modified from Brewster and Bodmer, and Merritt and Whitington (Brewster and Bodmer, 1995; Merritt and Whitington, 1995). da neurons, red diamonds; external sensory neurons, yellow circles; other multidendritic neurons, green triangles; chordotonal organs, blue rectangles. The lateral oenocytes are shown as gray ovals. We have designated names for the dorsal cluster neurons on the basis of their typical ventral to dorsal cell body position. (B) Gal4 109(2)80-driven mCD8::GFP in third instar md neurons, oenocytes and chordotonal organs. An arrow indicates the position of the neuron labeled in C.
(C; top) Components of the MARCM system used to characterize the normal morphologies of da neurons.
(Bottom) A mitotic clone of ddaD. (Its location within a typical hemisegment is indicated by a white arrow in B.)
(D) Computer tracings of the branching patterns of the four classes of neurons. Representative main branches and side branches from single neurons in each class are shown. These branches are not oriented according to larval axes.
Dorsal is up and anterior to the left in panels A-C. Scale bars, 100 μm (B); 50 μm (D).

suited for examining the molecular basis of dendritic morphogenesis and tiling. The PNS comprises defined cell types with characteristic dendritic projections (Zawarzin, 1912), including the type I neurons with ciliated monopolar dendrites and the type II neurons with multiple dendritic (md) projections (Fig. 1A). The md neurons of *Drosophila* have been further classified into three subtypes according to their substrate and morphology (Fig. 1A) (Bodmer and Jan, 1987); (1) the tracheal dendrite (md-td) neurons, (2) neurons with bipolar dendrites (md-bd) and (3) the dendritic arborization (md-da) neurons, which spread dendrites along the epidermis. Two lines of evidence suggest that dendritic tiling occurs among the md-da neurons. First, in *Drosophila* larvae, dendrites of the dorsal cluster neurons normally avoid projecting across the dorsal midline but will invade this territory if cells on the other side of the midline are ablated (Gao et al., 2000). Second, anatomical and physiological studies of individual larval da neurons in the moth *Manduca sexta* have shown that dendrites from morphologically similar, but non-homologous, neurons within a hemisegment innervate non-overlapping territories (Grueber et al., 2001). Together, these data indicate that the *Drosphila* PNS may be a fruitful system in which to explore the molecular basis of dendritic tiling.

We have undertaken studies in *Drosophila* to characterize the diversity of dendrite morphologies and the extent of dendritic tiling among the da neurons. We have used the MARCM system (Lee and Luo, 1999) to make single-cell clones and classify the da neurons into four morphological classes. By quantifying the dendritic territories of all neurons within each class, we show that two classes independently provide nearly complete body wall coverage. Careful examination of the dendritic territories of adjacent cells reveals that overlap is minimal when cells belong to the same class: where like dendrites are closely apposed they typically terminate or make abrupt turns instead of crossing over. Next, we asked if *starry night (stan)* and *sequoia (seq)*, two genes involved in limiting dendrite growth (Gao et al., 1999; Brenman et al., 2001), are required in a cell-autonomous fashion for such tiling. Our data suggest that cell-autonomous *seq* function is not essential for widespread tiling of the body wall. The situation with *stan* is more complex, as a low percentage of *stan* mutant neurons extended single sparsely branched processes beyond their normal dendritic territories.

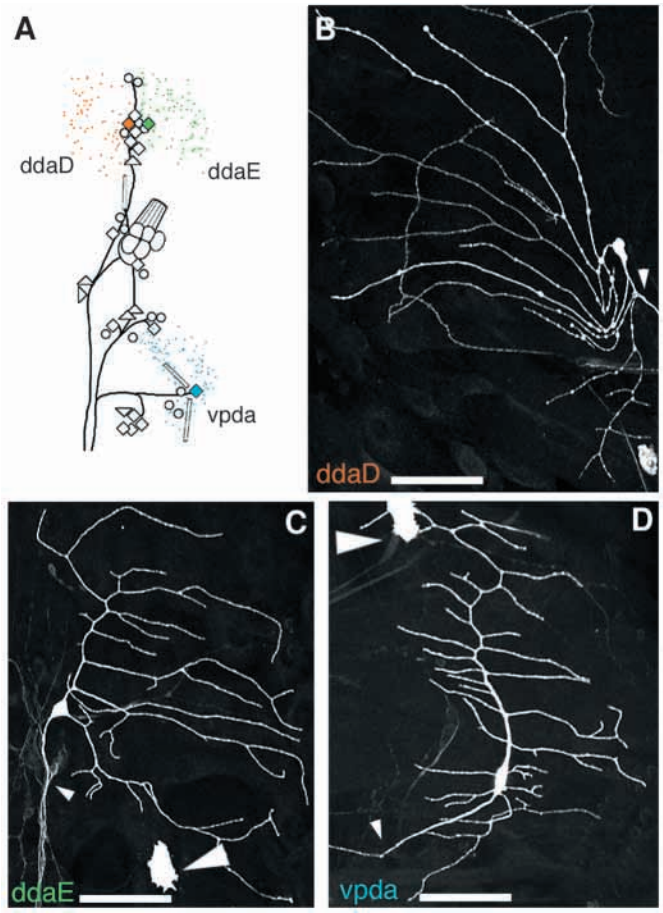

Fig. 2. Identities and dendritic morphologies of class I neurons. (A) Locations and territories of class I neurons in a schematized hemisegment of the abdominal PNS. Four cells were used to construct maps of each neuron in this and subsequent figures. Included in this class are ddaD (B; *n*=8), ddaE (C; *n*=10) and vpda (D; *n*=12). (B-D) Dendritic morphologies of ddaD (B), ddaE (C) and vpda (D). The name of the neuron in each confocal image is shaded the same color as its corresponding cell body and dendritic branch terminals in the PNS schematic (A). Axons are indicated by small arrowheads. Epidermal cells labeled by activity of the ELAV-Gal4 construct are indicated by a large arrowhead. Dorsal is up and anterior is to the left. Scale bars, 50 μm.

We discuss the relevance of this overextension phenotype to the problem of tiling and suggest that several as yet unidentified signals act to establish non-overlapping dendritic domains between like neurons in the *Drosophila* PNS.

MATERIALS AND METHODS

Drosophila stocks

The following stocks were used for MARCM analysis in this study: *w, ELAV-Gal4, hsFLP; FRTG13, tub-Gal80/CyO* (Lee and Luo, 1999), *yw; FRTG13, UAS-mCD8::GFP/CyO* (Lee and Luo, 1999), *w, ELAV-Gal4, hsFLP, UAS-mCD8::GFP* (Lee and Luo, 1999), *yw; FRT G13, tub-Gal80/CyO* and *yw; FRT42D, tub-Gal80* (kindly provided by Drs Liqun Luo and Haitao Zhu, Stanford University). For analysis of *seq* we used the stock *yw; FRT42D, seq^{22}/CyO* (Brenman et al., 2001). For analysis of *stan* we used *yw; FRTG13, fmi^{E59}/CyO* (Usui et al., 1999). In addition, the Gal4 insertion line 109(2)80 (Gao et al., 1999) was recombined with UAS-mCD8::GFP on the second chromosome to make a stock expressing mCD8::GFP in all da neurons.

MARCM labeling and immunocytochemistry

To identify and characterize the peripheral dendrites of each da neuron we used the MARCM system (Lee and Luo, 1999). For producing clones, females were provided with a freshly yeasted grape agar plate and allowed to lay eggs for 2 hours. Developing eggs were kept at 23-25°C and given a 37°C heat shock 3-5 hours after the end of the laying period. Two distinct heat shock regimes were used. For random labeling of small numbers of peripheral neurons for arbor reconstruction we subjected embryos to a single 1 hour heat shock. To examine the spatial relationships of arbors of neighboring neurons, we gave a 30 minute heat shock, followed by a 30 minute recovery period and a second 45 minute heat shock. The first method usually resulted in three to five labeled peripheral neurons per animal. The second method resulted in up to six labeled da neurons per hemisegment.

We identified GFP-labeled clones by examining living third instar larvae under a fluorescence microscope fitted with a 4× lens. Selected larvae were immersed in phosphate buffered saline (PBS; pH 7.4) and opened along the dorsal or ventral midline depending on the location of the labeled neuron. Filleted and pinned larvae were fixed with 3.7% formaldehyde for 1 hour at room temperature, rinsed several times in PBS with 0.3% Triton X-100 (PBS-TX) and blocked in 5% normal donkey serum (NDS; Jackson Laboratories, West Grove, PA). Primary antibodies were used at a concentration of 1:100 for rat anti-mCD8 (Caltag, Burlingame, CA) and 1:200 for mouse mAb 22C10 (Zipursky et al., 1984) and incubated overnight at 4°C. Secondary antibodies were Cy2 or Cy3-conjugated donkey anti-rat (diluted 1:200; Jackson Laboratories) and goat anti-mouse (diluted 1:500), respectively. After overnight incubation in secondary antibodies, the tissue was rinsed for several hours in PBS-TX, mounted on poly-L-lysine coated coverslips, dehydrated using an ethanol series (5 minutes each in 30%, 50%, 75%, 90%, 100% and 100%), cleared in xylenes (2×10 minutes) and mounted in DPX (Fluka, Milwaukee, WI). As an alternative to antibody staining, we imaged GFP fluorescence in living third instar larvae by cutting their posterior termini and mounting them in 90% glycerol.

Image processing and cell reconstruction

Our maps of the da system of the mature third instar larva are based on data from over 300 marked neurons in segments A2-A6. Representative clones were selected for detailed cell reconstructions on the basis of the quality and completeness of staining and the integrity of arbors following mounting. For cell reconstructions, 1 μm Z-series stacks were acquired on a Bio-Rad MRC-600 confocal microscope (Bio-Rad, Hercules, CA) using a 40× objective (1.3 n.a.), projected into a 2D image using COMOS software and assembled as montages in Photoshop 5.0 (Adobe Systems, San Jose, CA). Black and gray levels were typically adjusted to equalize the various images. Tracings of the neurons were made in Photoshop by adding a transparent layer and tracing the arbors using a mouse.

Quantitative analysis

We used the Strahler method (Strahler, 1953; Uylings et al., 1975) to order and analyze the branching patterns of the da neurons. Terminal branches were assigned an order of one. Where two first-order branches met, an order of two was assigned. Where two second-order branches met, an order of three was assigned and so on for the whole cell. If a lower order branch (i.e. one) met a higher order branch (i.e. two), the higher branch order was carried on without change. Once dendrites were ordered in such a manner, the assignments were reversed (Berry et al., 1975) so that extensions from the cell body became the lowest order branches and the terminals became the highest order branches.

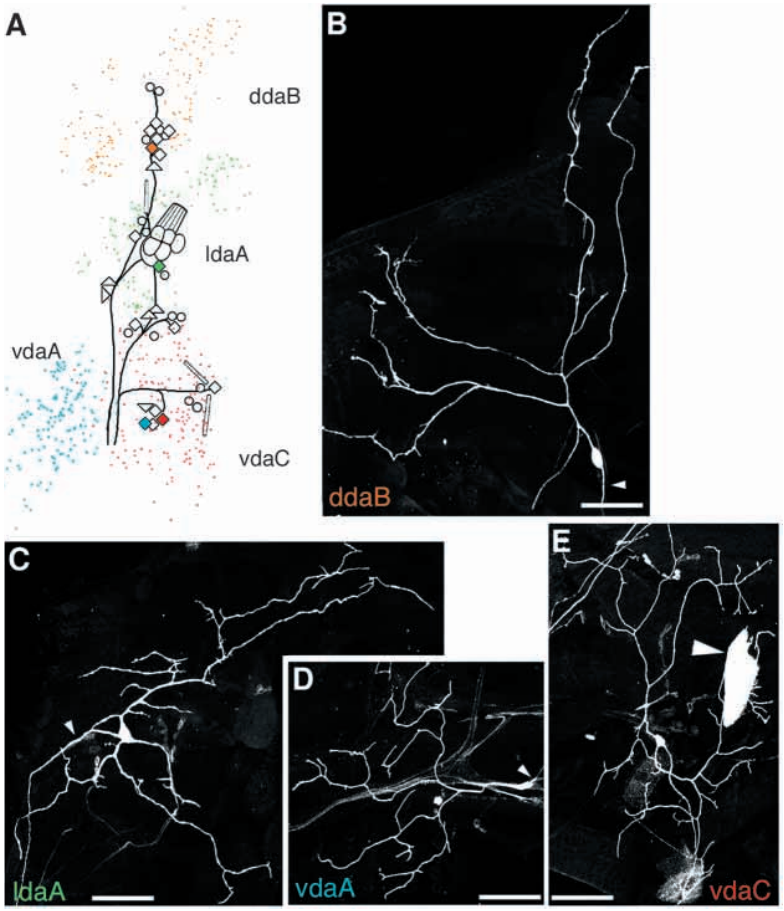

Fig. 3. Identities and dendritic morphologies of class II neurons. (A) Locations and dendritic territories of class II neurons in a schematized hemisegment of the abdominal PNS. Included in this class are ddaB (B; *n*=11), ldaA (C; *n*=16), vdaA (D; *n*=6) and vdaC (E; *n*=8). (B-E) Morphologies of individual class II neurons. The name of the neuron in each confocal image is shaded the same color as its corresponding cell body and dendritic branch terminals in the PNS schematic (A). Axons are indicated by small arrowheads. A labeled epidermal cell in E is indicated by a large arrowhead. Dorsal is up and anterior is to the left. Scale bars, 50 μm.

To quantify the dendritic field sizes of each neuron, Z-series files were acquired on a Leica (TCS SP2) confocal microscope using a 20× (0.7 n.a.) objective, projected into a 2D image and imported into Image Pro Plus (MediaCybernetics). Dendritic fields were delineated by a polygon connecting the distal-most dendritic tips or arcs. We used these same images to plot the dendritic terminals of each neuron manually in Photoshop using a mouse. Four plots of each cell were used to construct each of the four composite hemisegments. We standardized dendritic territory positions and orientations within a hemisegment by using the segment border and the lateral oenocytes as positional markers.

RESULTS

Morphological heterogeneity among the dendritic arborization neurons

The 15 dendritic arborization (da) neurons in hemisegments A2-A6 are arranged in four clusters (ventral, ventral′, lateral and dorsal; Fig. 1A). The nomenclature for the da neurons identifies their position within one of these four clusters with the prefix v, v', l or d, their status as a da neuron and an alphabetic suffix that orders the cells from ventral to dorsal within each cluster (Bodmer and Jan, 1987; Bodmer et al., 1989). Three neurons (vpda, v'ada and v'pda) do not conform to this naming scheme. In this study, we have named each neuron according to its typical position within a cluster; however, the primary criterion for identifying each cell is its peripheral dendritic morphology (see below). We identified four neurons grouped together in a ventral cluster (vdaA-D), one lone ventral neuron (vpda) (Bodmer and Jan, 1987), the previously identified v'ada and v'pda neurons (Bodmer and Jan, 1987), the two lateral neurons ldaA and ldaB and six dorsal da neurons (ddaA-F).

The da neurons together spread extensive overlapping dendrites across the epidermis (Fig. 1B). Viewed together, the pattern of dendrites covering each hemisegment appeared to be stereotyped from animal to animal, suggesting that each cell probably had a defined morphology and dendritic territory. To examine the dendritic morphologies of individual neurons in more detail, we produced wild-type mCD8::GFP-labeled clones using the MARCM system (Lee and Luo, 1999). The dendrites of da neurons were robustly labeled by inducing MARCM clones during embryogenesis and imaging these clones in third instar larvae (*n*=303 clones; Fig. 1C). Each individual da neuron had a characteristic branching pattern and territory across the epidermis. We identified four classes of branching patterns and found that each cell had dendrites that were entirely and consistently of one or another of these types. We term these class I, II, III and IV neurons (and dendrites), in order of increasing arbor complexity (Fig. 1D; Table 1). We examine each class in more detail below.

Dendritic branching patterns and territories of individual da neurons

Class I neurons

The class I neurons, including vpda, ddaD and ddaE, together innervated the dorsal region and a limited ventral region of each hemisegment (Fig. 2A). Each neuron had a relatively long dorsal-directed primary dendrite, which branched repeatedly along its length into secondary dendrites with anteroposterior orientations (Fig. 2B-D). ddaD was a moderate outlier from this group, as a branched dorsal-directed primary dendrite was not always clearly distinguishable, and its arbor often had a sparse fan-shaped appearance (Fig. 2B). Class I dendrites were smooth, with few side branches or varicosities. Strahler analysis showed that these neurons have the least complex branching patterns of the da neurons (Table 1).

Class II neurons

The class II da neurons are vdaA, vdaC, ldaA and ddaB (Fig. 3A). This class innervated most of the ventral region of each hemisegment, as well as portions of the lateral and dorsal body wall (Fig. 3A). The dendrites of each neuron were long and sinuous and typically more symmetrically bifurcating

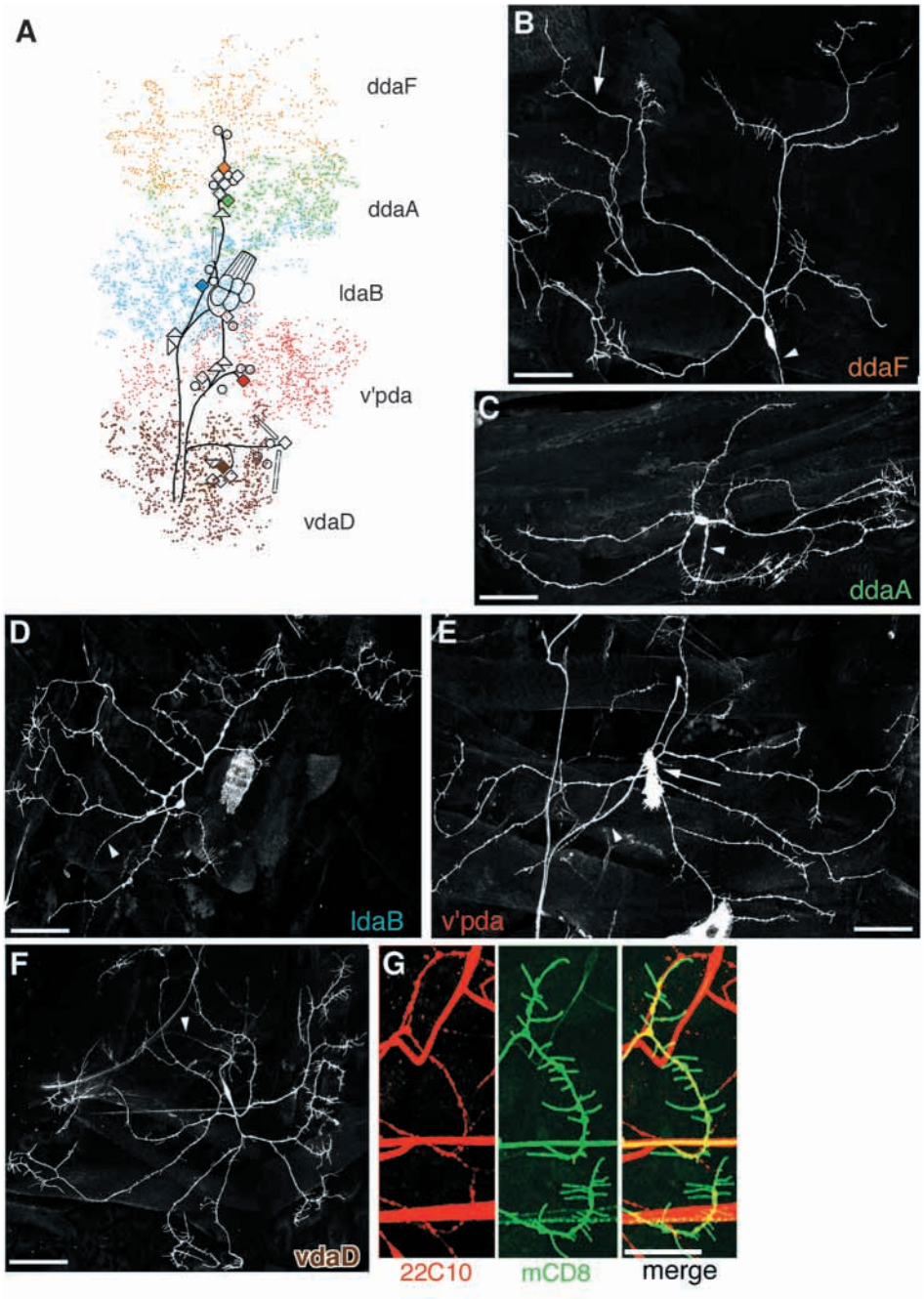

Fig. 4. Identities and dendritic morphologies of class III neurons. (A) Locations and dendritic territories of class III neurons in a schematized hemisegment of the abdominal PNS. Included in this class are ddaF (B; *n*=24), ddaA (C; *n*=13), ldaB (D; *n*=23), v'pda (E; *n*=22) and vdaD (F; *n*=12). (B-F) Morphologies of individual class III neurons. Axons are indicated by small arrowheads. The name of the neuron in each confocal image is shaded the same color as its corresponding cell body and dendritic branch terminals in the PNS schematic (A). The white arrow in B indicates the position of the segment border. To the left of this arrow, dendrites mix with a ddaE clone in the next anterior segment. An arrow in E indicates the position of the v'pda cell body between a labeled es neuron (above) and an epidermal cell (below). (G) Double labeling with mAB 22C10 to label axons and dendrites and anti-mCD8 to label a class III clone. Note the extensive spiked protrusions extending from primary trunks that are labeled by 22C10 (which labels a microtubule-binding protein) (Hummel et al., 2000). Dorsal is up and anterior is to the left. Scale bars, 50 μm.

than the class I dendrites, but they showed few higher order branches as they extended to distant targets (up to 350 μm from the cell soma in the case of ddaB) on the body wall (Fig. 3B-E). Higher order branches of these cells were generally only 1-5 μm stubs extending from the major trunks (Fig. 3). Although the dendrites of class I and class II neurons differed in the orientation of their processes and the sizes of their dendritic fields (Table 2), their complexities, as assessed by Strahler analysis, were not significantly different (Table 1).

Table 1. Reversed Strahler analysis of da neurons

Class	1st order	2nd order	3rd order	4th order	5th order
I	0.4 (±0.5)	2.4 (±0.9)	9.7 (±3.6)	31.4 (±10.4)	-
I (-ddaD)	0.75 (±0.5)	3.0 (±0.8)	12.0 (±2.9)	38.3 (±8.1)	-
II	1.5 (±0.5)	4.3 (±1.3)	12.8 (±4.3)	49.8 (±12.7)	-
III	1.0 (±0.0)	3.5 (±0.6)	11.8 (±1.3)	32.8 (±7.9)	371 (±61.4)

The means (±s.d.) number of branches in each order is shown. The following neurons were analyzed as many times as indicated in the parentheses: Class I, ddaD (3), ddaE (2), vpda (2); Class II, ddaB (1), ldaA (1), vdaC (1), vdaA (1); Class III, ddaA (1), ldaB (1), vdaD (2).

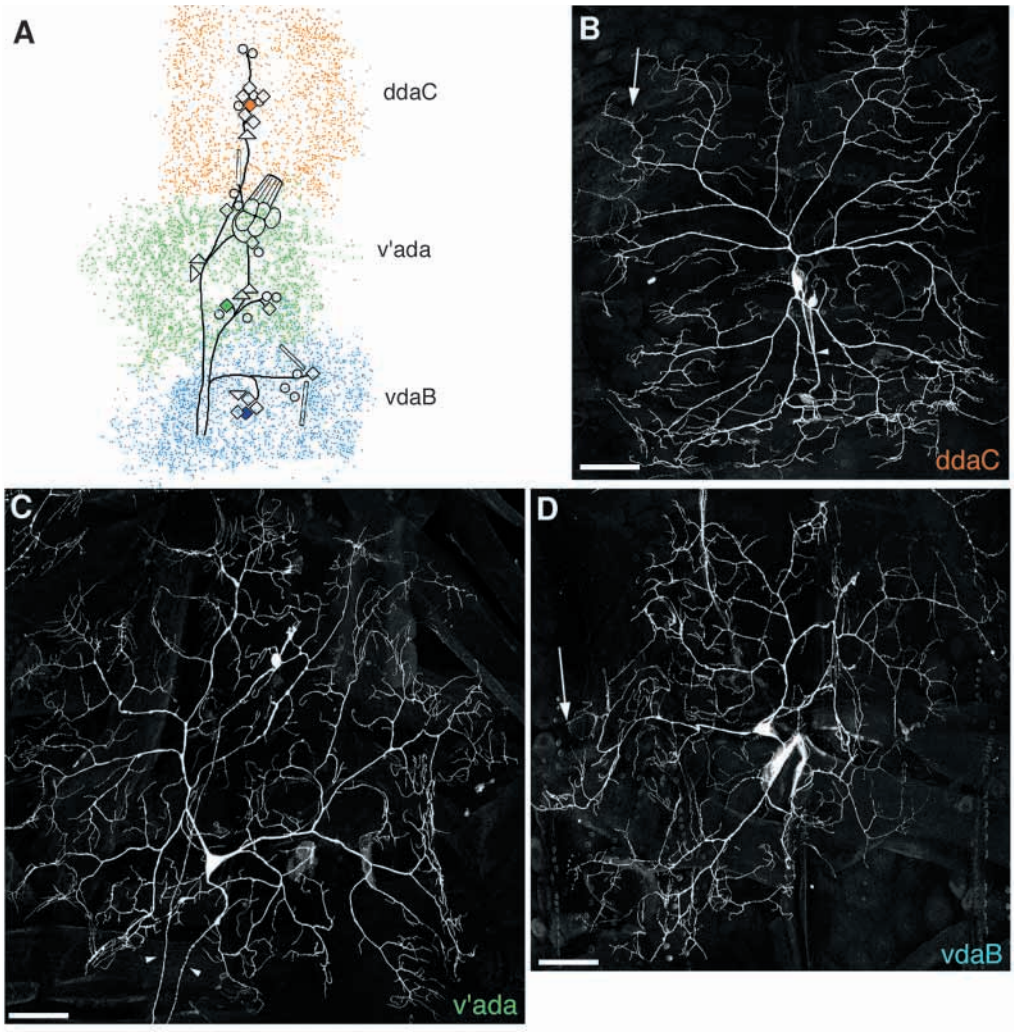

Fig. 5. Identities and dendritic morphologies of class IV neurons. (A) Locations and dendritic territories of class IV neurons in a schematized hemisegment of the abdominal PNS. Included in this class are ddaC (B; *n*=63), v'ada (C; *n*=46) and vdaB (D; *n*=29). Overlap of terminals in the map represents cell-to-cell variation in field size rather than a violation of tiling (see Results). (B-D) Morphologies of individual class IV neurons. Axons are marked by small arrowheads. The name of the neuron in each confocal image is shaded the same color as its corresponding cell body and dendritic branch terminals in the PNS schematic (A). The arbor of each cell covers an entire region of the body wall from the anterior to posterior segment boundaries (arrows in B and D). Dorsal is up and anterior is to the left. Scale bars, 50 μm.

Class III neurons

Class III neurons were the most numerous of the four classes and included vdaD, v'pda, ldaB, ddaA and ddaF (Fig. 4A). Together the territories of these neurons covered approximately 70% of each abdominal hemisegment (Fig. 4A; Table 2). Class III dendrites were characterized by long primary and secondary branches (Fig. 4B-F) similar to those of the class II dendrites. However, class III dendrites were clearly distinguished by having spiked protrusions (1-20 μm long) along most of their length (Fig. 4G) and at the ends of their major dendritic trunks. The branching complexity of class III neurons was significantly higher than class I and class II neurons owing to these numerous spiked extensions (Table 1).

Class IV neurons

The class IV neurons included vdaB, v'ada and ddaC (Fig. 5). These neurons together provided a segmental coverage that approached 100% (Fig. 5A; Table 2). Class IV dendrites showed a highly complex branching pattern that completely filled large regions of the body wall with arbors. Mature high-order branches showed evidence of isoneuronal (same cell) avoidance, as they often terminated or turned before crossing each other (Fig. 5B-D). Class IV neurons were not analyzed by the Strahler method because slight folds in the epidermis distorted the pattern of connectivity of terminal dendrites. A sampling of individual trunks, however, indicated that each of these cells has as many as 800-900 terminal branches, and more than six branch orders (data not shown), thereby clearly distinguishing them from the three other da classes.

Extensive dendritic overlap among neurons in different classes

Relatively little is known about how the dendritic territories of neurons are established during development. The *Drosophila* da system is advantageous for addressing this issue because arbors branch in two dimensions and thus can be imaged in their entirety (Bodmer and Jan, 1987; Gao et al., 1999). For the da neurons, cell ablation experiments have shown that dendritic exclusion occurs between homologous cell clusters at the dorsal midline and thus limits dorsal dendrite extension (Gao et al., 2000). Anatomical data from individual neurons in *Manduca sexta* suggest that dendritic exclusion occurs at the midline and also, more generally, helps to shape the territories innervated by the different da neurons (Grueber et al., 2001).

To begin to investigate the factors that control da neuron territory formation in *Drosophila*, we characterized patterns of overlap and non-overlap between pairs of identified neurons and related these results to the morphological classes of the

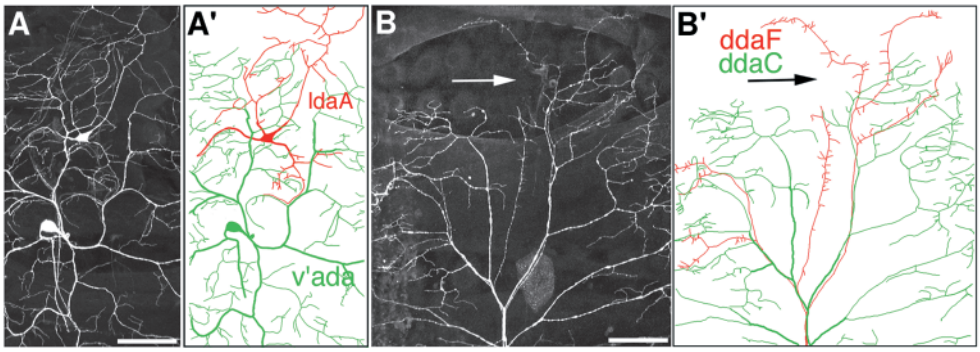

Fig. 6. Dendrites in different classes overlap extensively. (A,A′) A confocal image of v'ada (class IV; green in A′) and ldaA (class II; red in A′) which were dually labeled using the MARCM system. (B,B′) Branches belonging to the dorsal cluster neurons ddaC (class IV; green in B′) and ddaF (class III; red in B′) typically extend along the same path. The main dendritic trunks of each neuron emerge at the bottom of the panel (the cell bodies are just out of view). The dendrites of ddaC terminate near the dorsal midline (arrow), but those of ddaF extend into the contralateral hemisegment. Dorsal is up and anterior is to the left. Scale bars, 50 μm.

neurons (according to the above classification scheme). By using a repeated heat shock MARCM protocol (see Materials and Methods), we induced simultaneous labeling of several neurons in each hemisegment. These clones revealed that, depending on their spatial proximity, neighboring neurons of different morphologies could show either extensive overlap or complete overlap of their dendritic fields (Fig. 6A,B). We found no evidence for stratification of morphologically different dendrites (the distance between dendrites in the Z-direction was typically less than 1 μm); thus overlapping dendrites essentially branched in a 2D space. Furthermore, primary branches of adjacent neurons often followed the same initial paths (Fig. 6B,B′). These regions of dendritic association typically concluded with one of the dendrites turning abruptly and the other continuing along its prior trajectory (Fig. 6B,B′), suggesting that one of the neurons received a stop signal to which the other did not respond.

We were unable to assess the overlap of class I and class II neurons because we did not identify a dual label of two adjacent cells. Nevertheless, our data support the general conclusion that dendritic exclusion does not occur between da neurons that have distinct dendritic morphologies.

Table 2. Dendritic field sizes and epidermal coverage by da neurons

Class	Neuron	n	Average dendritic area (μm^2)	Hemisegment coverage (%)
I				14-17
	vpda	5	19900	
	ddaD	6	28500	
	ddaE	3	18500	
II				33-39
	vdaA	6	26100	
	vdaC	5	37700	
	ldaA	4	34200	
	ddaB	6	56700	
III				63-74
	vdaD	5	58200	
	v'pda	6	57100	
	ldaB	8	54800	
	ddaA	6	39700	
	ddaF	4	86400	
IV				86-101
	vdaB	6	106400	
	v'ada	5	141800	
	ddaC	6	157800	

Two-dimensional projections of confocal images of each neuron were averaged by tracing distal arbor boundaries. The hemisegment coverage was calculated by summing the average territories of each neuron and dividing by an average ±s.d. (giving upper and lower coverages) hemisegmental area for third instar larvae (taken from seven representative segments).

Lack of dendritic overlap among cells of the same morphological class

Whereas neurons in different classes often cluster together and project dendrites to overlapping regions of the epidermis, cells in the same class were more evenly spaced across the body wall and projected dendrites to distinct domains (Fig, 2A, Fig. 3A, Fig. 4A, Fig. 5A). To examine whether like dendrites partially overlapped or, on the contrary, were excluded from each other's territories, we examined patterns of dendritic overlap between neurons of the same morphological type. Maps of the territories of class I and class II neurons (Fig. 2A, Fig. 3A) and a single dual label of adjacent ventral class II neurons (Fig. 7A,A′) show that, within each class, dendrites are non-overlapping. However, these dendrites typically extended to regions of the body wall that were non-contiguous, and thus terminal dendrites of different cells were not usually found in close proximity.

As the territories of adjacent class III and class IV cells were contiguous (Fig. 4A, Fig. 5A), these neurons provided a more rigorous test of whether the dendrites of like neurons are excluded from each other's territories. For the class III neurons, we identified six cases in which adjacent neurons were co-labeled by the MARCM technique. In each case, the arbors of the two neurons approached each other but did not overlap. Distal heteroneuronal branches (those belonging to different cells) of the same class either bent away from each other or terminated before crossing (Fig. 7B,C). The only apparent exception to this rule was a short dorsal-directed branch of ddaA that overlapped with the cell body and a proximal trunk of ddaF (Fig. 4C) (data not shown). We also observed exclusion when one cell was labeled using the MARCM system and an adjacent cell was labeled with the 22C10 antibody (data not shown). These data, together with maps of the territories of each neuron (Fig. 4A) and a calculated body wall coverage factor (Table 2) indicate that the class III neurons together provide non-redundant and majority coverage of the epidermis.

We identified a total of 21 cases in which two or three adjacent class IV neurons (vdaB, v'ada, or ddaC) were labeled. The arbors of vdaB and v'ada met approximately midway between their cell bodies (Fig. 7D,D′), whereas the dendrites

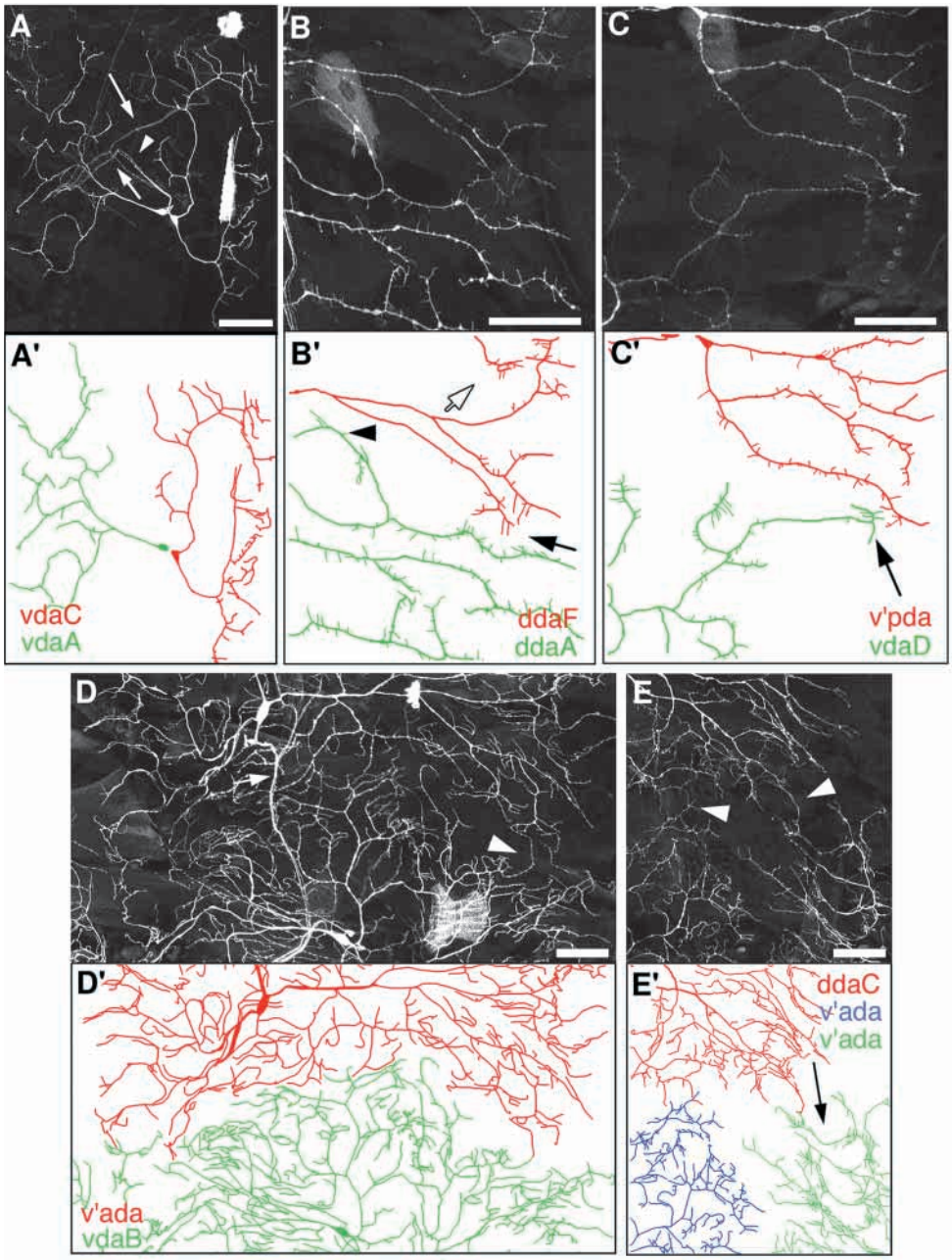

Fig. 7. Dendrites of adjacent class II (A), III (B,C) and IV (D,E) neurons do not overlap. (A,A′) Dual labeling of the class II neurons vdaA and vdaC. White arrows indicate labeling of motoneurons, and a white arrowhead indicates the axons of vdaA and vdaC. (B,C) Lack of overlap between dendrites of class III neurons (*n*=6). Examples of dendritic exclusion between dorsal cluster neurons (ddaA and ddaF; B) and ventral neurons (v'pda and vdaD; C) are shown. The confocal images (B,C) are color coded (B′,C′) to identify the individual branches of each neuron. A white arrow in B′ shows an example of avoidance between dendrites of the same neuron (isoneuronal avoidance). Black arrows in B′ and C′ show cases in which a dendrite from one cell terminates its growth before crossing the dendrite of an adjacent cell. A black arrowhead in B′ shows a dendrite that turns away from the dendrites of an adjacent cell. (D,E) Class IV dendrites from adjacent neurons form non-overlapping boundaries (*n*=21). Examples of dendritic exclusion between v'ada and vdaB (D; dendrites are colored in D′) and ddaC and v'ada segmental homologs (E; dendrites are colored in E') are shown. A white arrow in D shows the axon of v'ada extending to the CNS. White arrowheads in D and E show points of apparent dendritic contact and/or crossing. In these cases, the cell of origin of each dendrite branch was difficult to determine unambiguously. A black arrow in E′ shows the location of the segment border. Dorsal is up and anterior is to the left in all panels. Scale bars, 50 μm.

of v'ada and ddaC met at the lateral margin near the oenocytes (Fig. 7E,E′). Dendrites of these adjacent pairs typically crossed once along their borders (Figs 7, 8), but along the rest of the border dendritic exclusion was the rule (Fig. 7D,E). These boundaries did not obviously correlate with physical boundaries such as muscle insertion sites. The dendritic exclusion between these neurons also occurred at segment boundaries (between both homologous and non-homologous pairs of neurons; Fig. 7E,E′) and at the dorsal and ventral midlines (data not shown).

In summary, tiling between distinct but morphologically alike neurons results in the formation of two complete mappings of the larval body wall. Tiling occurs between da neurons in different sensory cell clusters and, in the case of the dorsal cluster class III neurons, between neurons in the same cluster.

MARCM analysis of the roles of *starry night* and *sequoia* in tiling

Studies of the *starry night* (*stan*) gene suggest that it is required for dendritic exclusion between homologous neurons at the dorsal midline and may act in a cell-autonomous fashion (Gao et al., 2000). We examined whether *stan* is required for widespread tiling of the body wall by using the MARCM system to produce mCD8::GFP-labeled da neurons carrying the $stan^{E59}$ allele (Fig. 9A). In each single-cell clone examined (*n*=23), most dendrites formed defined boundaries where they would normally encounter the dendrites of adjacent neurons (Fig. 9B,C). In two out of 11 class IV neurons, we observed one or two unbranched dendrites that showed an abnormally long projection (Fig. 9D,E). In one case observed in the dorsal cluster, the branch did not invade the territory of the contralateral hemisegment but, rather, projected aberrantly along the dorsal midline to the anterior adjacent segment. In the other case, the ventral cluster class IV neuron showed sinuous unbranched dorsal

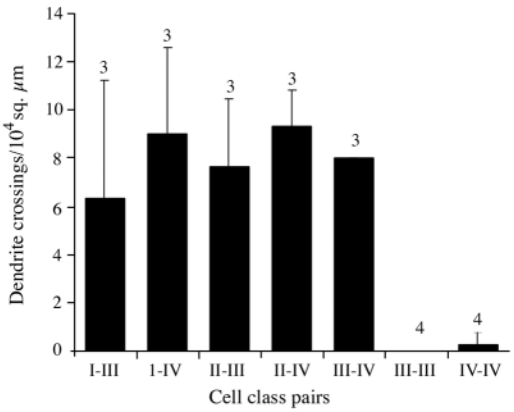

Fig. 8. Quantification of dendritic crossing among different cell pairs within a randomly chosen 10^4 μm^2 area where the territories of two adjacent cells meet. Overlap was not quantified for class I or II dendrites because we did not observe co-labelings of adjacent neurons (see Results). The means±s.d. are shown. The numbers above each bar indicate *n* values.

and ventral overextensions that terminated as tufts of dendrites beyond the cell's territory proper (Fig. 9D,E). The remaining branches of these neurons appeared to terminate at their normal locations on the body wall (Fig. 9D,E).

Another gene that could participate in tiling is *sequoia* (*seq*), a zinc-finger protein that acts as a pan-neuronal regulator of axon and dendrite morphogenesis (Brenman et al., 2001). Because *seq* mutants show an overgrowth of dendrites in the dorsal PNS cluster (Gao et al., 1999), we made MARCM clones to examine specifically whether *seq* might regulate tiling. *seq* mutant external sensory (es) neurons showed morphological defects, such as dendrite splitting, as has been previously described (Brenman et al., 2001). The class-specific branch morphologies of individual da neurons, however, were preserved in *seq* clones. Morphological defects appeared not to disrupt the typical dendritic field of the da neurons that we examined (*n*=28 neurons with representatives from each class). Furthermore, where dendrites of adjacent class IV neurons met, normal exclusion was observed (Fig. 9F).

DISCUSSION

The *Drosophila* da system comprises morphologically distinct classes of sensory neurons

We have identified the peripheral dendritic morphologies of da neurons in the *Drosophila* abdominal PNS and have established four morphologically distinct types of cells, which we term class I, II, III and IV neurons. These morphological distinctions were robust, as the branch morphology of each cell consistently placed it into the same class. In addition, the distinct branch morphologies did not reflect transient developmental states, as we observed morphological distinctions between neurons in all larval stages examined (data not shown).

Our morphological characterization of *Drosophila* da neurons indicates that they are similar to the da neurons of the moth *Manduca sexta*, of which there are at least three distinct morphological classes (Grueber et al., 2001). In *Manduca*, the alpha, beta and gamma da neurons show morphological similarities to the class I/II, IV and III da neurons of *Drosophila*, respectively. *Manduca* alpha neurons appear to function as proprioceptors, whereas gamma neurons probably function as touch receptors (Grueber et al., 2001). Whether the *Drosophila* da neurons are functionally similar to *Manduca* da neurons remains to be determined. At least two lines of evidence, however, suggest that the morphological classes that we have identified in *Drosophila* represent functionally distinct types of neurons. First, *pickpocket* (*ppk*), a degenerin/epithelial sodium channel subunit (Adams et al., 1998; Darboux et al., 1998), appears to be expressed only in the class IV neurons ddaC, v'ada and vdaB (W. G., B. Ye, L. Y. J., Y. N. J., unpublished). As *ppk* may have a physiological role in mechanotransduction (Adams et al., 1998), its expression in class IV neurons could underlie a functional specialization of these cells. Second, *Drosophila* da neurons have dichotomous axonal projections, which probably reflect their functional distinctions (Merritt and Whitington, 1995; Schrader and Merritt, 2000). Most da neurons project into the ventral neuropil (Schrader and Merritt, 2000), a characteristic of tactile projections (Murphey et al., 1989). vpda and an unidentified neuron in the dorsal cluster, by contrast, have more dorsal projections (Merritt and Whitington, 1995; Schrader and Merritt, 2000), which is similar to proprioceptive neurons (Pflüger et al., 1988; Murphey et al., 1989). The ventral-projecting neurons appear to correspond to the class II, III and IV neurons, whereas the dorsal projections belong to at least a subset of the class I neurons.

Genetic specification of the da neurons

An important issue arising from our characterization of the *Drosophila* da system is how the morphological properties of each neuron relate to their genetic specification. Previous studies have shown that the *Drosophila* da system consists of genetically distinct subgroups of neurons (Dambly-Chaudiere and Ghysen, 1987; Blochlinger et al., 1990; Jarman et al., 1993; Merritt and Whitington, 1995; Brewster and Bodmer, 1995). Most da neurons require proneural genes in the *achaete-scute* complex (ASC) (Dambly-Chaudiere and Ghysen, 1987) arise as components of external bristle lineages (Brewster and Bodmer, 1995; Orgogozo et al., 2001), and express the Cut protein (Blochlinger et al., 1990). The only da neurons that do not share these characteristics are vpda and two dorsal neurons. vpda remains in ASC-mutant embryos but is lost in animals mutant for the proneural gene, *atonal* (Jarman et al., 1993). One dorsal da neuron requires a third proneural gene, *amos* (Huang et al., 2000; Brewster et al., 2001). Finally, vpda and two dorsal da neurons fail to express Cut (Blochlinger et al., 1990).

Reconciling these accumulated data with our cell-by-cell characterization of the da system, it appears that the class II, III and IV neurons are those that require *ASC* genes and express Cut. Class I neurons, on the other hand, do not express detectable levels of Cut (W. B. G., L. Y. J., Y. N. J., unpublished) and could correspond to the da neurons that require *atonal* and/or *amos* (although only one *ASC*-independent neuron has been described in the dorsal cluster). Consistent with these assignments, during our mosaic analysis we often observed class III and class IV neurons co-labeled with es neurons (see Fig. 4E and 5B, respectively), suggesting

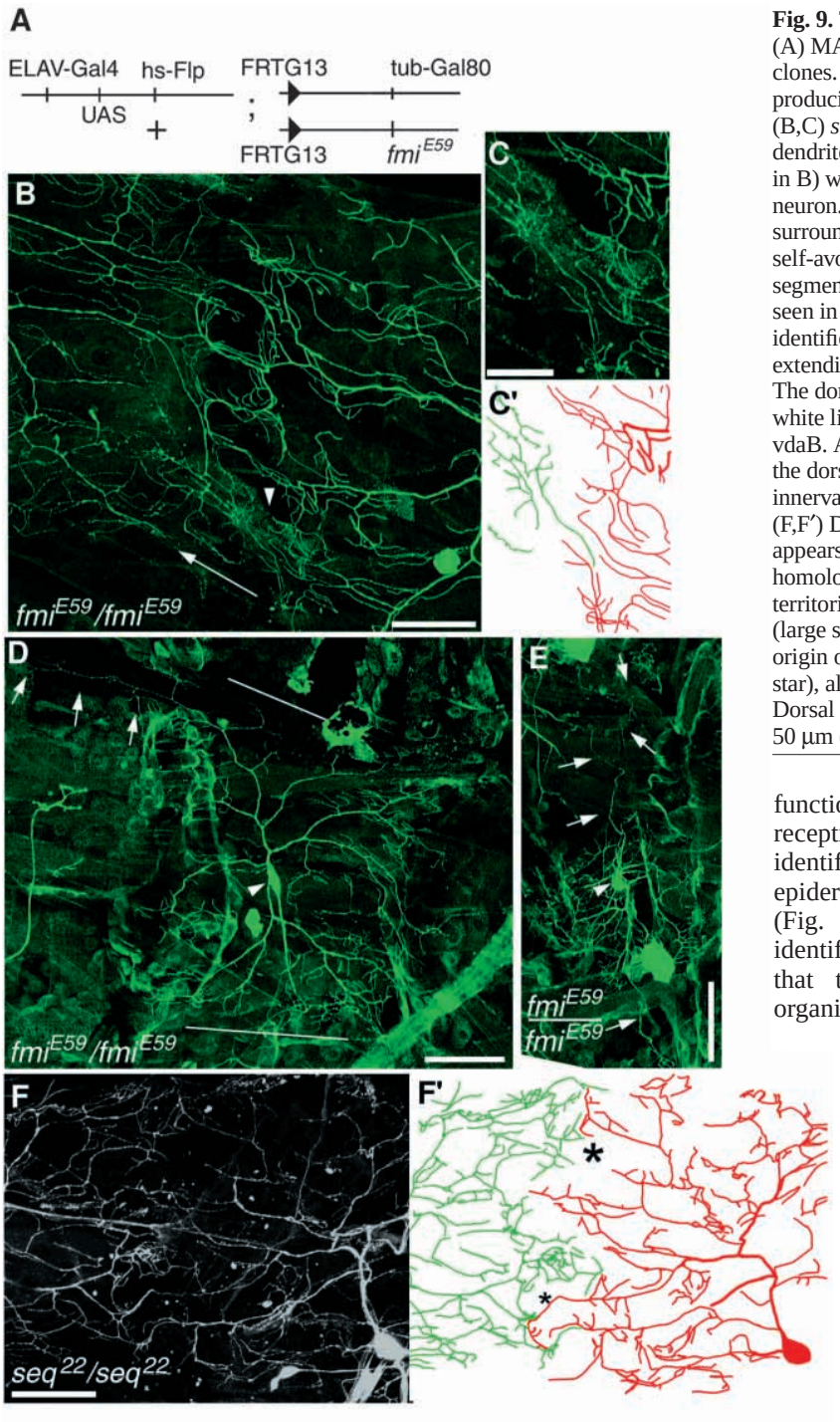

Fig. 9. Tiling in *stan*^{E59} (*fmi*^{E59}) and *seq*^{22} mutant neurons. (A) MARCM scheme for producing *stan*^{E59} (*fmi*^{E59}) mutant clones. 'UAS' indicates a UAS-mCD8::GFP insertion. For producing *seq* clones FRT42D was used in place of FRTG13. (B,C) *stan*^{E59}/*stan*^{E59} (*fmi*^{E59}/*fmi*^{E59}) segmental homologs. The dendrites of these ddaC neurons stop at the lateral margin (arrow in B) where they meet the dendrites of an adjacent class IV neuron. (C,C′) A high-magnification view of the region surrounding the arrowhead in B, where dendrites show normal self-avoidance and are excluded from the territory of a segmental homolog. (D) Dendritic overextension phenotype seen in a *stan* (*fmi*) mutant ddaC neuron. A white arrowhead identifies the cell body. The white arrows identify a branch extending beyond the segment border along the dorsal midline. The dorsal and ventral boundaries of the cell are delineated by white lines. (E) Dendritic overextension in the ventral neuron, vdaB. A white arrowhead identifies the cell body. Arrows follow the dorsal and ventral extensions. The remaining branches innervate their normal territory in the ventral body wall. (F,F′) Dendritic field formation by *seq*^{22}/*seq*^{22} type IV neurons appears normal. As shown here, dendrites of v'ada segmental homologs (traced in red and green in F′) avoid each other's territories and form normal boundaries at the segment border (large star). In some areas near the segment border, the cell of origin of individual dendrites is difficult to determine (small star), although obvious dendrite crossing was not observed. Dorsal is up and anterior is to the left. Scale bar, 25 μm (C,C′); 50 μm (B,F,F′); 100 μm (D,E).

that these cells could have arisen from a common precursor. The class II neurons are likely also es related because all four neurons in the ventral cluster are lineally related to es organs (Orgogozo et al., 2001) and two class II neurons reside here (Fig. 3). Understanding how the genes required for early da specification are linked to the activation of distinct programs of dendritic morphogenesis is an important goal for future studies.

Morphologically alike da neurons tile the epidermis

Tiling is a principle of dendrite organization in which functionally similar neurons completely fill available receptive territories with little or no redundancy. We have identified two independent tilings of the *Drosophila* epidermis by da neurons bearing similar morphologies (Fig. 7). A similar type of tiling has recently been identified in *Manduca* (Grueber et al., 2001), suggesting that this is an evolutionarily conserved plan for organizing the da sensory system. In *Drosophila*, tiling occurs between class III da neurons and between class IV da neurons, which each partitions the body wall into a collection of non-overlapping territories (Fig. 7). Furthermore, class III and IV neurons each provide a nearly complete segmental coverage (Table 2). Dendrites with distinct morphologies, by contrast, can cross extensively (Figs 6, 8).

The tiling of the *Drosophila* epidermis by class III and IV neurons appears analogous to the tiling among physiologically alike vertebrate retinal ganglion cells. In this system, ON-center and OFF-center, four ON-OFF direction-selective classes and several other cell types, including amacrine cells, provide independent tilings of the retina (Wässle et al., 1981; Wässle and Boycott, 1991; Amthor and Oyster, 1995; MacNeil and Masland, 1998). Such an arrangement ensures that each region of the visual field is 'viewed' by each physiological type of ganglion cell. Additionally, as visual information is distributed to the appropriate centers of the brain, the location of its origin is unambiguous, thereby maintaining a coherent representation of sensory space. The same rules of organization applied to the insect da system would likewise be advantageous. Mechanical and thermal stimuli often necessitate rapid and finely directed behavioral responses, particularly when they could lead to

damage to the cuticle (Frings, 1945; Walters et al., 2001). If future studies show that the da neurons comprising each tiling class are united by their physiology, as we suspect, then these modalities would have the capacity to provide accurate spatial resolution of stimuli landing anywhere on the body wall.

What mechanisms and molecules control dendritic tiling?

Although the cellular mechanisms that control dendritic tiling are not yet understood, several developmental scenarios can be envisioned. Individual dendrites could repel like dendrites where they meet. Alternatively, neurons could be endowed with a limited capacity for dendritic growth (depending, for example, on cell size) and form their territories without influence from neighboring neurons. Finally, in the case of the da neurons, interactions with the epidermis or surrounding tissue, such as muscle, could provide permissive or restrictive growth signals. These mechanisms are not mutually exclusive and could conceivably act in concert. In the da system, however, dendritic boundaries could not always be correlated with physical boundaries, such as muscle insertion sites, and terminal dendrites typically turned abruptly where they met like dendrites. Thus, our data do not provide strong support for the latter two mechanisms (limited growth capacity and physical boundaries) but do suggest that branch interactions could contribute to tiling. Experimental studies of the effects of adding neurons to, and removing neurons from, the da system will provide essential tests of the importance of these mechanisms. Additionally, because our data are taken from mature da neurons, a crucial question still to be addressed is how dendrites of like neurons behave during development as their territories are established. Dendrites could show exclusion throughout their development or, alternatively, refine their boundaries as a maturational step.

Regulation of tiling by dendritic branch interactions is a likely scenario in the vertebrate retina, where contact-mediated avoidance signals appear to operate in a cell-type-specific manner (Wässle et al., 1981; Amthor and Oyster, 1995; Hitchcock, 1989). Furthermore, morphological data from mammalian retinal neurons show that dendro-dendritic contacts are made between like neurons but not between unlike neurons (Lohmann and Wong, 2001). Such contacts could provide an opportunity for these neurons to signal to each other by their activity or cell surface composition (Lohmann and Wong, 2001). Similarly, we typically observed single apparent dendritic contacts between tiling class IV neurons. Whether these contacts are important for exclusion among the remaining branches remains to be determined.

The molecular mechanisms of dendritic tiling in the vertebrate retina have not been established. Mutant screens of the second chromosome in *Drosophila* (Gao et al., 1999) (D. Cox, W. G., G. Tavosanis, L.Y. J., Y. N. J., unpublished) might be informative in this regard, as several candidate loci have been identified that cause early overextension of dendrites. We have tested alleles of two of these genes, *stan* (Gao et al., 2000) and *seq* (Brenman et al., 2001), for possible roles in tiling. In seq^{22} and $stan^{72}$ mutant embryos, dendrites show an overextension phenotype and exhibit abnormal crossing of the dorsal midline (Gao et al., 2000; Brenman et al., 2001). Our MARCM analysis using the seq^{22} and $stan^{E59}$ alleles suggests that such overextension might not reflect a widespread defect in dendritic exclusion, because a majority of the dendrites terminate or turn where contact with an adjacent like neuron occurs or would be expected (compare Fig. 5A with Fig. 9B-E). Importantly, however, one or two sparsely branched processes were seen extending beyond the normal boundary of the cell in 18% of the class IV *stan*-mutant neurons (Fig. 9D,E).

If branch recognition and exclusion are required for tiling, which appears to be the case for the class IV neurons (this study), one interpretation of the *stan* phenotype is that the dendrite is overextending because it does not receive or transduce a repulsive signal that requires Stan function. Alternatively, because in wild-type neurons exclusion occurs among terminal dendritic branches (Fig. 7), a lack of exclusion in *stan*-mutant neurons could arise if the overextended processes are equivalent to primary trunks and thus lack the machinery for tiling. However, without information about the fields of surrounding like neurons, we cannot eliminate the possibility that exclusion is intact in *stan*-mutant neurons. By extending earlier, or more rapidly, than the rest of the dendritic field (Gao et al., 2000), these single processes could have successfully invaded an uninnervated region of the body wall. This latter scenario seems to provide a reasonable explanation for why we observed a dorsal branch from ddaC overextending along the dorsal midline (one of the last regions of the body wall to become innervated; Fig. 9D). Whether a similar 'invasion' scenario could account for the overextended processes from vdaB (Fig. 9E) might ultimately depend on the timing and pattern of outgrowth of its class IV neighbors (i.e. how far can a dendrite of a $stan^{-}$ vdaB neuron extend before encountering like dendrites?). Because our MARCM experiments suggest that *stan* acts cell autonomously in the dendritic arborization neurons, future studies might be conducted using cell-type specific markers of the class IV neurons in a *stan* (and *seq*) mutant background. Such markers would allow the visualization of all neurons together and, as a result, provide a better indication of the relationship between early dendritic overextension phenotypes and tiling.

Could similar mechanisms regulate isoneuronal and heteroneuronal dendritic exclusion?

In addition to the dendritic exclusion that occurs between like neurons, we frequently observed exclusion between dendrites that belong to the same neuron (Figs 2-5). Such 'self-avoidance' has been identified in *Manduca* sensory neurons (Grueber and Truman, 1999; Grueber et al., 2001) and characterized experimentally in leech sensory axons (Yau, 1976; Kramer and Kuwada, 1983; Kramer and Stent, 1985; Gan and Macagno, 1995; Wang and Macagno, 1998; Baker et al., 2000); however the underlying mechanisms are not understood. In theory, self-avoidance and tiling might not require distinct signals or signaling pathways (among like neurons) because isoneuronal dendrites could be developmentally identical to 'like' heteroneuronal dendrites. It will therefore be of special interest to compare the mechanisms of exclusion by isoneuronal and heteroneuronal branches during development. Ultimately, an understanding of the distinction between these two processes will require the elucidation of their molecular underpinnings.

We thank Liqun Luo, Haitao Zhu, Jay Brenman and the Bloomington Stock Center for providing fly stocks, Tadashi Uemura

for the gift of Flamingo antibodies, members of the Jan lab for discussions and criticism, Susan Younger for advice about genetics and Anhthu Hoang and Gaia Tavosanis for comments on the manuscript. W. B. G. thanks James Truman for generously supporting preliminary work on this project. Supported by NIH 1R01 NS 40929-0 to Y. N. J., NIH NS 29971 to J. W. T., and NIH T32 NS007-067-23 to W. B. G., Y. N. J. and L. Y. J. are Investigators of the Howard Hughes Medical Institute.

REFERENCES

Adams, C. M., Anderson, M. G., Motto, D. G., Price, M. P., Johnson, W. A. and Welsh, M. J. (1998). Ripped pocket and pickpocket, novel *Drosophila* DEG/ENaC subunits expressed in early development and mechanosensory neurons. *J. Cell Biol.* **140**, 143-152.

Amthor, F. R. and Oyster, C. W. (1995). Spatial organization of retinal information about the direction of image motion. *Proc. Natl. Acad. Sci. USA* **92**, 4002-4005.

Baker, M. W., Rauth, S. J. and Macagno, E. R. (2000). Possible role of the receptor protein tyrosine phosphatase HmLAR2 in interbranch repulsion in a leech embryonic cell. *J. Neurobiol.* **45**, 47-60.

Berry, M., Hollingsworth, T., Anderson, E. M. and Flinn, R. M. (1975). Application of network analysis to the study of the branching patterns of dendritic fields. *Adv. Neurol.* **12**, 217-245.

Blochlinger, K., Bodmer, R., Jan, L. Y. and Jan, Y. N. (1990). Patterns of expression of Cut, a protein required for external sensory organ development in wild-type and *cut* mutant *Drosophila* embryos. *Genes Dev.* **4**, 1322-1331.

Bodmer, R. and Jan, Y. N. (1987). Morphological differentiation of the embryonic peripheral neurons in *Drosophila*. *Roux's Arch. Dev. Biol.* **196**, 69-77.

Bodmer, R., Carretto, R. and Jan, Y. N. (1989). Neurogenesis of the peripheral nervous system in *Drosophila* embryos: DNA replication patterns and cell lineages. *Neuron* **3**, 21-32.

Brenman, J. E., Gao, F. B., Jan, L. Y. and Jan, Y. N. (2001). Sequoia, a tramtrack-related zinc finger protein, functions as a pan-neuronal regulator for dendrite and axon morphogenesis in *Drosophila*. *Dev. Cell* **1**, 667-677.

Brewster, R. and Bodmer, R. (1995). Origin and specification of type II sensory neurons in *Drosophila*. *Development* **121**, 2923-2936.

Brewster, R., Hardiman, K., Deo, M., Khan, S. and Bodmer, R. (2001). The selector gene *cut* represses a neural cell fate that is specified independently of the *Achaete-Scute* Complex and *atonal*. *Mech. Dev.* **105**, 57-68.

Dambly-Chaudiere, C. and Ghysen, A. (1987). Independent subpatterns of sense organs require independent genes of the *achaete-scute* complex in *Drosophila* larvae. *Genes Dev.* **1**, 297-306.

Darboux, I., Lingueglia, E., Pauron, D., Barbry, P. and Lazdunski, M. (1998). A new member of the amiloride-sensitive sodium channel family in *Drosophila melanogaster* peripheral nervous system. *Biochem. Biophys. Res. Commun.* **246**, 210-216.

Frings, H. (1945). The reception of mechanical and thermal stimuli by caterpillars. *J. Exp. Zool.* **99**, 115-139.

Gan, W. B. and Macagno, E. R. (1995). Interactions between segmental homologs and between isoneuronal branches guide the formation of sensory terminal fields. *J. Neurosci.* **15**, 3243-3253.

Gao, F. B., Brenman, J. E., Jan, L. Y. and Jan, Y. N. (1999). Genes controlling dendrite outgrowth, branching, and routing in *Drosophila*. *Genes Dev.* **13**, 2549-2561.

Gao, F. B., Kohwi, M., Brenman, J. E., Jan, L. Y. and Jan, Y. N. (2000). Control of dendritic field formation in *Drosophila*: the roles of Flamingo and competition between homologous neurons. *Neuron* **28**, 91-101.

Grueber, W. B. and Truman, J. W. (1999). Development and organization of a nitric-oxide-sensitive peripheral neural plexus in larvae of the moth, *Manduca sexta*. *J. Comp. Neurol.* **404**, 127-141.

Grueber, W. B., Graubard, K. and Truman, J. W. (2001). Tiling of the body wall by multidendritic sensory neurons in *Manduca sexta*. *J. Comp. Neurol.* **440**, 271-283.

Hitchcock, P. F. (1989). Exclusionary dendritic interactions in the retina of the goldfish. *Development* **106**, 589-598.

Huang, M.-L., Hsu, C.-H. and Chien, C.-T. (2000). The proneural gene *amos* promotes multiple dendritic neuron formation in the *Drosophila* peripheral nervous system. *Neuron* **25**, 57-67.

Hummel, T., Krukkert, K., Roos, J., Davis, G. and Klambt, C. (2000). *Drosophila* Futsch/22C10 is a MAP1B-like protein required for dendritic and axonal development. *Neuron* **26**, 357-370.

Jan, Y. N. and Jan, L. Y. (2001). Dendrites. *Genes Dev.* **15**, 2627-2641.

Jarman, A. P., Grau, Y., Jan, L. Y. and Jan, Y. N. (1993). *atonal* is a proneural gene that directs chordotonal organ formation in the *Drosophila* peripheral nervous system. *Cell* **73**, 1307-1321.

Kramer, A. P. and Kuwada, J. Y. (1983). Formation of the receptive fields of leech mechanosensory neurons during embryonic development. *J. Neurosci.* **3**, 2474-2486.

Kramer, A. P. and Stent, G. S. (1985). Developmental arborization of sensory neurons in the leech *Haementeria ghilianii*. II. Experimentally induced variations in the branching pattern. *J. Neurosci.* **5**, 768-775.

Lee, T. and Luo, L. (1999). Mosaic analysis with a repressible cell marker for studies of gene function in neuronal morphogenesis. *Neuron* **22**, 451-461.

Lohmann, C. and Wong, R. O. L. (2001). Cell-type specific dendritic contacts between retinal ganglion cells during development. *J. Neurobiol.* **48**, 150-162.

MacNeil, M. A. and Masland, R. H. (1998). Extreme diversity among amacrine cells: Implications for function. *Neuron* **20**, 971-982.

Masland, R. H. (2001). The fundamental plan of the retina. *Nat. Neurosci.* **4**, 877-886.

Merritt, D. J. and Whitington, P. M. (1995). Central projections of sensory neurons in the *Drosophila* embryo correlate with sensory modality, soma position, and proneural gene function. *J. Neurosci.* **15**, 1755-1767.

Murphey, R. K., Possidente, D. A., Pollack, G. and Merritt, D. J. (1989). Modality-specific axonal projections in the CNS of the flies *Phormia* and *Drosophila*. *J. Comp. Neurol.* **290**, 185-200.

Orgogozo, V., Schweisguth, F. and Bellaïche, Y. (2001). Lineage cell polarity, and *inscutable* function in the peripheral nervous system of the *Drosophila* embryo. *Development* **128**, 631-643.

Perry, V. H. and Linden, R. (1982). Evidence for dendritic competition in the developing retina. *Nature* **297**, 683-685.

Pflüger, H. J., Braunig, P. and Hustert, R. (1988). The organization of mechanosensory neuropils in locust thoracic ganglia. *Phil. Trans. R. Soc. B Lond.* **321**, 1-26.

Schrader, S. and Merritt, D. J. (2000). Central projections of *Drosophila* sensory neurons in the transition from embryo to larva. *J. Comp. Neurol.* **425**, 34-44.

Scott, E. K. and Luo, L. (2001). How do dendrites take their shape? *Nat. Neurosci.* **4**, 359-365.

Strahler, A. N. (1953). Revisions of Horton's quantitative factors in erosional terrain. *Trans. Am. Geophys. Un.* **34**, 345.

Usui, T., Shima, Y., Shimada, Y., Hirano, S., Burgess, R. W., Schwarz, T. L., Takeichi, M. and Uemura, T. (1999). Flamingo, a seven-pass transmembrane cadherin, regulates planar cell polarity under the control of Frizzled. *Cell* **98**, 585-595.

Uylings, H. B. M., Smit, G. J. and Veltman, W. A. M. (1975). Ordering methods in quantitative analysis of branching structures of dendritic trees. *Adv. Neurol.* **12**, 247-254.

Walters, E. T., Illich, P. A., Weeks, J. C. and Lewin, M. R. (2001). Defensive responses of larval *Manduca sexta* and their sensitization by noxious stimuli in the laboratory and field. *J. Exp. Biol.* **204**, 457-469.

Wang, H. and Macagno, E. R. (1998). A detached branch stops being recognized as self by other branches of a neuron. *J. Neurobiol.* **35**, 53-64.

Wässle, H. and Boycott, B. B. (1991). Functional architecture of the mammalian retina. *Physiol. Rev.* **71**, 447-478.

Wässle, H., Peichl, L. and Boycott, B. B. (1981). Dendritic territories of cat retinal ganglion cells. *Nature* **292**, 344-345.

Weber, A. J., Kalil, R. E. and Stanford, L. R. (1998). Dendritic field development of retinal ganglion cells in the cat following neonatal damage to visual cortex: evidence for cell class specific interactions. *J. Comp. Neurol.* **390**, 470-480.

Yau, K. W. (1976). Physiological properties and receptive fields of mechanosensory neurones in the head ganglion of the leech: comparison with homologous cells in segmental ganglia. *J. Physiol.* **263**, 489-512.

Zawarzin, A. (1912). Histologische Studien uber Insekten. II Das sensible Nervensystem der Aeschnalarven. *Z. Wess. Zool.* **100**, 245-286.

Zipursky, S. L., Venkatesh, T. R., Teplow, D. B. and Benzer, S. (1984). Neuronal development in the Drosophila retina: monoclonal antibodies as molecular probes. *Cell* **36**, 15-26.